2000-GT-518

A CFD MODEL FOR REAL GAS FLOWS

Carlo Cravero - Antonio Satta
DIMSET - Università di Genova
via Montallegro n.1 - 16145 Genova
ITALIA

ABSTRACT

Numerical solutions of Navier-Stokes equations are nowadays widely used for several industrial applications in different fields (aerodynamic, propulsion, naval, combustion, etc..), but the solution methods still require significant improvements especially in two aspects: turbulence modeling and fluid modeling. The paper describes in some detail a real fluid model based on Redlich-Kwong-Aungier equation of state and its implementation into a Navier-Stokes solver developed by the authors for turbomachinery flows analysis.

NOMENCLATURE

a, b, c	RKA equation coefficients
C_{ax}	blade axial chord
c_v, c_s	constant volume specific heat, sound speed
delta	boundary layer thickness
e, $\overline{e}$	internal energy, total energy
F,G	mass, momentum and energy flux vectors
F_v, G_v	diffusive flux vectors
h	enthalpy
L	duct length
Ma_{is}	isentropic mach number
n	RKA equation coefficient
p	static pressure
Pr_l, Pr_t	laminar and turbulent Prandtl numbers
Q	conservative flow variables vector
R	gas constant
Re	Reynolds number
RK	Redlich-Kwong
RKA	Redlich-Kwong-Aungier
sn	normal distance from the wall
t, T	time, static temperature
u, v	Cartesian components of velocity
v, V	specific volume, velocity (sqrt(u^2+v^2))
x, y,	Cartesian co-ordinates
Z	compressibility factor

Greek

μ_l, μ_t	laminar and turbulent viscosities
ρ	density
ω	acentric factor

Subscript

c	critical point value
e	external to the boundary layer
R	reduced value (divided by critical point value)
t	total quantity
1,2	inlet, outlet sections

Superscript

0	ideal gas value

INTRODUCTION

CFD techniques are currently used in industry for design purposes in many different fields (i.e. propulsion, chemistry, combustion etc…). The importance of such numerical methods for the integration of Navier-Stokes equations is steadily growing because of their increasing reliability and flexibility; in fact the same numerical scheme can be applied to solve different flows provided the appropriate set of boundary conditions is implemented. This is particularly true for gas turbines flow analysis where transonic flows with strong viscous effects (compressor first stages) or heat exchange (turbine) or subsonic flows (compressor last stages) and combustion (combustion chamber) are encountered.

Three main paths in CFD modelling research can nowadays been highlighted: a) flexible and robust schemes for steady or unsteady flows at all speeds (matrix preconditioning, higher order time-integration schemes, ...), b) turbulence modelling (2 equations, Reynolds stress, ...), c) fluid properties modelling (two phase, real gas, cryogenics, ...). In the paper a contribution to the third class of problems is described.

Different flow models, to account for real gas effects, have been proposed and two main categories can be fairly clearly distinguished: analytical equations of state and numerical curve fitting of experimental tables.

The main advantages of an equation of state is to keep a reasonably good accuracy in a quite large range of pressures and temperatures for many substances. On the other hand curve fitting can give a higher accuracy level but the model must be tuned for a specific fluid.

Another aspect to be considered in a CFD model is the computation time required to evaluate thermodynamic parameters such as enthalpy, internal energy or entropy; this is particularly true for a Navier-Stokes code where thermodynamic variables are computed from ten to twenty times for a single point and by considering that a single turbomachinery row calculation requires about 20k mesh points in 2D and 100k in 3D. With an explicit time marching scheme at least 5000 iterations are required for a steady flow analysis giving rise to an order of magnitude of 10^9 thermodynamic properties evaluations. An increase in computation time to predict thermodynamic parameters can have a significant effect on the computational efficiency of the Navier-Stokes code.

Several curve fitting technique have been proposed for the most common "industrial fluids", air and steam; this interpolating techniques have also been optimised for iterative calculations (Young, 1988, Patek, 1996, Srinivasan, 1987). The model from Young (1988) have been introduced into a throughflow code for multistage steam turbine analysis (Denton, 1978) that is routinely used in industrial practice. Nevertheless the throughflow method is a simplified 2D flow analysis that is much less computationally demanding than a 2D Navier-Stokes calculation.

Many equations of state have been presented and reviewed for different applications (Sullivan, 1981, Hall, 1980, Aungier, 1995). A good candidate equation of state should require a minimum number of (easy to find) data to clearly define the fluid and a sufficient accuracy in a wide range of applications. Considering that an equation of state requires less computational time to evaluate thermodynamic properties than curve fitting and that the same model can be used for many different fluids, it has been decided to choose the Redlich-Kwong equation of state, recently modified by Aungier (1995), because it keeps a better accuracy in comparison to the others reviewed equations and requires the critical point data only.

In the past several real gas models have been introduced into CFD codes (Glaister 1988, Grossman et al. 1989, Liou et al. 1990, Vinokur et al. 1990, Abgral 1991, Suresh et al. 1991,

Anderson 1992), but mainly for inviscid flow computations with high resolution schemes in 1D or 2D simple geometry.

In this work the implementation of the real gas model into a Navier-Stokes code, developed by the authors for turbomachinery applications, is presented. The need for such a research effort in CFD modelling is important for high pressure steam turbine stages, turbomachinery with cryogenic fluids and combustion. The code is validated against available 1D and 2D test cases and a preliminary steam turbine nozzle calculation is presented as well.

The attention is focused on the model implementation into the Navier-Stokes code.

REAL FLUID MODEL: THERMODYNAMIC

The Redlich-Kwong-Aungier (RKA) equation of state (Aungier, 1995) has the following expression:

$$p = \frac{RT}{v-b+c} - \frac{aT_R^{-n}}{v(v+b)} \tag{1}$$

where

$$a = 0.42747 \frac{R^2 T_C^2}{p_C} \qquad b = 0.08664 \frac{RT_C}{p_C}$$

$$c = \frac{RT_C}{p_C + \dfrac{a}{v_C(v_C+b)}} + b - v_C$$

Substance	T_c (K)	p_c (MPa)	Z_c	ω
Acetylene	309.5	6.24008	0.274	0.190
Ammonia	405.6	11.3962	0.245	0.255
Argon	151.0	4.86240	0.290	-0.002
Carbon Dioxide	304.2	7.38477	0.274	0.225
Carbon Oxide	133.0	3.49485	0.294	0.049
Ethanol	516.3	6.38190	0.248	0.635
Ethylene	283.1	5.11565	0.270	0.087
Helium	5.25	0.22800	0.320	-0.464
Hydrogen	33.25	1.29000	0.330	-0.220
Methane	190.7	4.63954	0.290	0.013
Methanol	513.2	7.95205	0.220	0.556
n-pentane	469.5	3.37329	0.269	0.252
Nitrogen	126.2	3.39355	0.291	0.040
Oxygen	154.8	5.07513	0.293	0.021
Propane	369.9	4.2546	0.277	0.152
Steam	647.3	22.0834	0.233	0.344
Xeno	289.8	5.8754	0.290	0.002

Tab.1 : Critical point data and acentric factors

The additional constant c has been introduced by Aungier to eliminate a weakness of the standard Redlich-Kwong model at

the critical point. As discussed by Aungier (1995) this addition does compromise the thermodynamic stability condition; nevertheless eq.1 becomes exact at the critical point and the constant c, being about two orders of magnitude smaller than b, has no significant effects far from the critical conditions. The most significant modification is the introduction of the general parameter n, instead of the fixed value 0.5. The optimum values of n can be well correlated by the following empirical function:

$$n = 0.498 + 1.1735\omega + 0.4754\omega^2$$

The acentric factor $\omega = -\log(p_{vR})$ is evaluated at $T_R = 0.7$.

g.1: Hydrogen - calculated vs experimental values
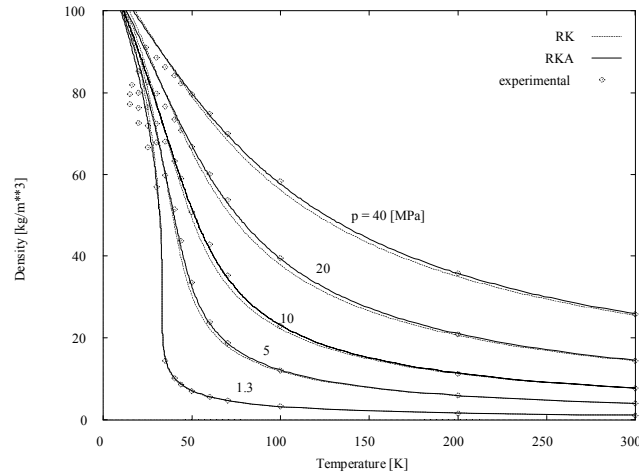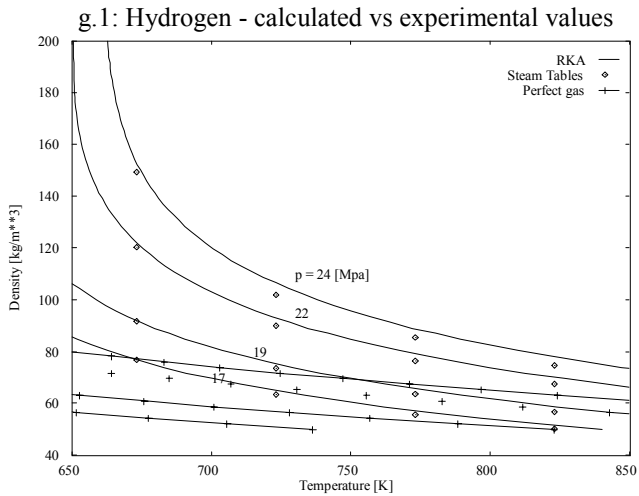
Fig.2: Steam - calculated vs experimental values

The value of the specific volume at the critical point can be calculated from the corresponding values of critical pressure and temperature using the compressibility factor Z_c. In Tab.1 critical point data for several substances of technical interest can be found. This data are obtained from Aungier (1995), Abbott et al. (1972) and Kirillin et al. (1987).

The predicted values of thermodynamic quantities (i.e. density, temperature, pressure) using eq.1 have been compared to the experimental (tabulated) values for hydrogen and steam in

order to verify the accuracy of the RKA equation. In fig.1-2 the density-temperature diagram for several isobar are plotted for hydrogen and steam respectively. The pressure values have been selected in a range applicable to turbomachinery flows (cryogenic pumps or steam turbines). In fig.1 the experimental values for hydrogen (from McCarty R.H., 1975) are compared to the calculated ones using the standard Redlich-Kwong (RK) and RKA equations. The pressure-temperature values are in the range for aerospace propulsion turbomachinery. The RKA equation gives a better representation of the thermodynamic state of the fluid. In fig.2 the calculated values (RKA) to the tabulated ones (standard steam tables) are compared in the pressure-temperature range of high pressure steam turbine stages. As is evident from fig.2 the perfect gas assumption, in these conditions, is clearly inadequate. After the preliminary analysis of the accuracy of the RKA equation in representing the thermodynamic state of typical fluids in turbomachinery application range, an analytical procedure has been applied to eq.1 in order to calculate the basic thermodynamic quantities and relations needed by a Navier-Stokes solver. Following the analytical procedure proposed by Bober and Chow (1990), the following set of functions has been obtained:

- *constant volume specific heat:*

$$c_v = c_v^0 + n(n+1)\frac{a}{b}T^{-1}T_R^{-n}\ln(1+b\rho) \qquad (2)$$

- *internal energy*

$$e = e^0 - \frac{a}{b}(n+1)T_R^{-n}\ln(1+b\rho) \qquad (3)$$

- *sound speed:* $\qquad (4)$

$$c_s^2 = \frac{RTv^2}{(v-b+c)^2} +$$

$$\frac{RTv^2}{c_v(v-b+c)}\left[\frac{R}{(v-b+c)} + nT_R^{-(n+1)}\frac{a}{v(v+b)}\right] +$$

$$- T_R^{-n}\frac{a(2v+b)}{(v+b)^2} +$$

$$nT_R^{-(n+1)}\frac{aTv}{c_v(v+b)}\left[\frac{R}{(v-b+c)} + nT_R^{-(n+1)}\frac{a}{v(v+b)}\right]$$

compressibility factor:

$$Z^3 + Z^2(c\frac{p}{RT} - 1) +$$

$$Z\frac{p^2}{(RT)^2}\left[b(c-b) - b\frac{RT}{p} + \frac{a}{p}T_R^{-n}\right] + \qquad (5)$$

$$\frac{p^2}{(RT)^3}a(c-b)T_R^{-n} = 0$$

3

Copyright (C) 2000 by ASME

The enthalpy is calculated from its definition: $h = e + p/\rho$.

The values of c_v and e are obtained from the corresponding values of the perfect gas. A polynomial variation of c_v^0 with temperature has been assumed according to Johnson (1965).
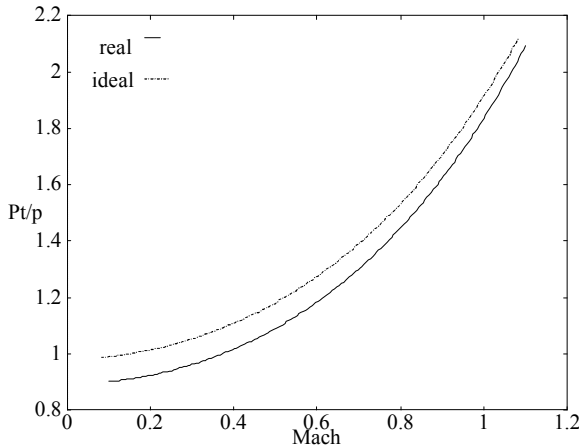
Fig.3: Hydrogen; total-to-static pressure
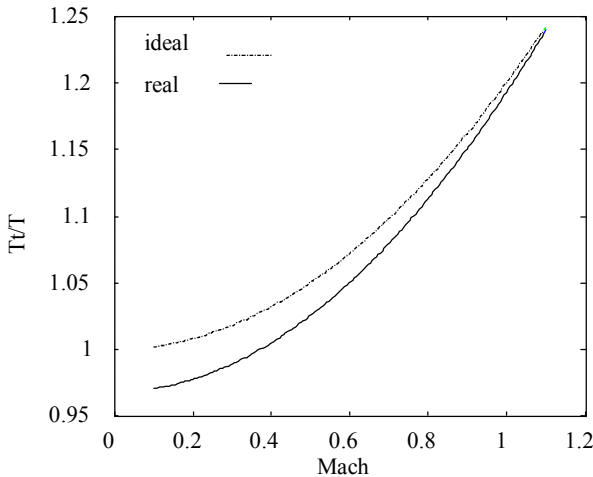
Fig.4: Hydrogen; total-to-static temperature

A basic relation for CFD is that for calculating total from static quantities (and vice versa). The following expression has been derived to compute total temperature (defined through an isentropic transformation) from static quantities :

$$\left.\frac{\partial T}{\partial \rho}\right|_S = \frac{T}{\rho^2 c_v}\left(\frac{R\rho}{1 - b\rho + c\rho} + nT^{-(n+1)}\frac{a\rho^2}{(1 + b\rho)T_C^{-n}}\right) \quad (6)$$

The above equation has been integrated using a Runge-Kutta method to compare the isentropic relations for ideal gases to the present real gas model. In fig.3-4 the relations for pressure and temperature for hydrogen are respectively shown. Static quantities are calculated from reference total values of $T_t=150$ [K] and $p_t=10$ [Mpa].

In fig.5-6 the total-to-static relations for steam with reference values of $T_t=800$ [K] and $p_t=20$ [Mpa] are plotted against the Mach number for the ideal and the real gas models.
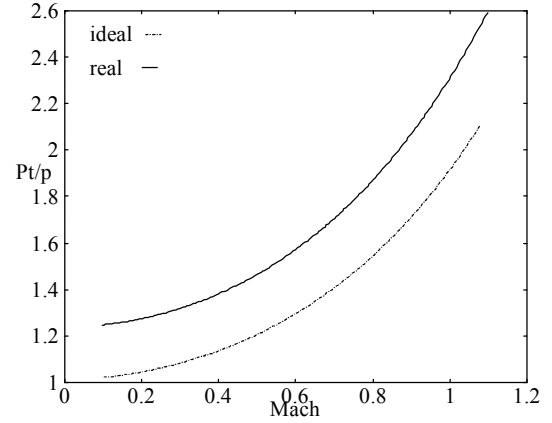
Fig.5: Steam; total-to-static pressure

In both cases the ideal and real gas models disagree. For the hydrogen case the average relative error ((real-ideal)/real) is about 8% for pressure and 2% for temperature. For the steam case the average relative error is about 7% for pressure and 2.7% for temperature.

Moreover the two cases show an opposite trend in the difference: in the example using hydrogen the quantities with the ideal gas model are overestimated, while in the example using steam the opposite occurs. This means that a general behavior of ideal vs real gas model cannot be defined and a real gas model is needed whenever the implementation of the perfect gas model is suspicious.
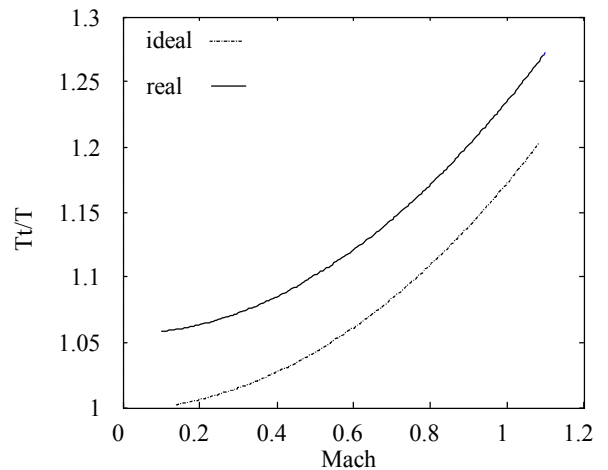
Fig.6: Steam; total-to-static temperature

It should be also noted that a total temperature inaccurate calculation in turbomachinery applications means a bad work exchange or heat transfer evaluation, while an erroneous total pressure computation gives unreliable values for losses.

4   Copyright (C) 2000 by ASME

NAVIER-STOKES SOLVER

An existing Navier-Stokes solver, previously developed by the authors for perfect gas flows (Chiari et al.,1998), has been modified to introduce the above real fluid model. The Reynolds-averaged equations are written in standard conservative form:

$$\frac{\partial}{\partial t}Q + \frac{\partial}{\partial x}F + \frac{\partial}{\partial y}G = \frac{1}{Re}\left(\frac{\partial}{\partial x}F_v + \frac{\partial}{\partial y}G_v\right) \qquad (7)$$

where

$$Q = \begin{pmatrix} \rho \\ \rho u \\ \rho v \\ \rho \bar{e} \end{pmatrix} \qquad F = \begin{pmatrix} \rho u \\ \rho u^2 + p \\ \rho uv \\ \rho u h_t \end{pmatrix} \qquad G = \begin{pmatrix} \rho v \\ \rho uv \\ \rho v^2 + p \\ \rho v h_t \end{pmatrix}$$

$$F_v = \begin{pmatrix} 0 \\ \tau_{xx} \\ \tau_{xy} \\ \Pi_x \end{pmatrix} \qquad G_v = \begin{pmatrix} 0 \\ \tau_{xy} \\ \tau_{yy} \\ \Pi_y \end{pmatrix} \qquad (8)$$

and

$$\Pi_x = \tau_{xx}u + \tau_{yx}v + \frac{\mu}{(\gamma-1)\,Pr}\frac{\partial}{\partial x}\left(c^2\right)$$

$$\Pi_y = \tau_{xy}u + \tau_{yy}v + \frac{\mu}{(\gamma-1)\,Pr}\frac{\partial}{\partial y}\left(c^2\right) \qquad (9)$$

$$\frac{\mu}{Pr} = \frac{\mu_l}{Pr_l} + \frac{\mu_t}{Pr_t}$$

The stress tensor is computed in the standard way using Stokes's hypothesis. The "total" energy per unit mass $\bar{e}$ in vector Q is defined as: $\bar{e} = e + \frac{1}{2}V^2$ (10)

A cell-vertex finite volume technique with an explicit Runge-Kutta integration method and Jameson artificial dissipation scheme has been used (Cravero et al., 1995a-b).
A Baldwin-Lomax algebraic turbulence model (Baldwin-Lomax, 1978) is implemented to compute the turbulent viscosity.

The control volume shown in fig.7 is considered; the conservative variables are stored in the grid vertices (black circle) while the diffusive terms are calculated in the auxiliary midpoints (white rectangular). This arrangement simplifies the computation of boundary points keeping a good accuracy with skewed grids.
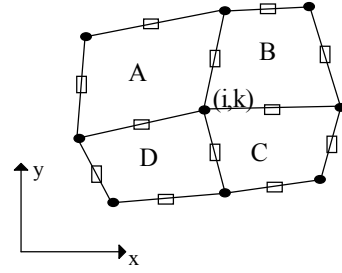
Fig.7: Control volume

The introduction of a different equation of state into the present solver is quite straightforward and this is one of the main advantages of explicit schemes with artificial dissipation over implicit or upwind based schemes. In fact the core of the solver is unchanged (it doesn't require any Jacobian matrix evaluation); an iterative procedure to obtain temperature from internal energy (eq.3) is required in order to compute static pressure from eq.1. A special attention is focused on boundary conditions at inlet and outlet. This is described in the next section. Standard periodicity conditions for turbomachinery applications with H-type grids are considered.

Inlet and outlet boundary conditions

The most significant modifications in the above Navier-Stokes solver are introduced to update inlet and outlet sections. Different set of quantities can be fixed at inlet or outlet according to the axial inlet Mach number. For turbomachinery computations it is known that the best set of values to fix is composed by: total pressure, total temperature and flow angles at the inlet and static pressure at the outlet. This is for subsonic inlet axial velocity, while for supersonic inlet Mach number an additional quantity is fixed at the inlet and all the values are extrapolated at the outlet.

At the inlet, in case of axial Mach number less than unity, total pressure, total temperature and flow angle are fixed and the static density is extrapolated from the interior point. To update all the conservative variables in the first axial section, the following procedure has been set up. The known values of p_{t1} and T_{t1} are substituted into eq.5 and the corresponding value of Z is obtained solving numerically (Newton-Raphson method) the cubic equation. The total density can be computed ($\rho_{t1} = p_{t1} / ZRT_{t1}$) and the static temperature is obtained by integrating eq.6 from point (T_{t1},ρ_{t1}) to (T_1,ρ_1). From eq.1-3 static pressure and internal energy are calculated. To update the "total" internal energy an additional relation is required. At this point it should be noted that the quantity $\bar{e}$ does not equal the internal energy (eq.3) calculated with T_t and ρ_t. In fact, the following thermodynamic definitions hold irrespective of fluid model:

5

Copyright (C) 2000 by ASME

$$h_t = h + \frac{1}{2}V^2 \qquad h = e + \frac{p}{\rho} \qquad (11)$$

From the above equations :

$$\bar{e} = e + \frac{1}{2}V^2 = e_t + \frac{p_t}{\rho_t} - \frac{p}{\rho} \qquad (12)$$

where e_t is the internal energy (eq.3) computed using the total values of T and ρ. From eq.12 the axial velocity u is obtained and all the conservative variables at the inlet can be computed. In case of supersonic inlet axial velocity all the quantities are fixed at inlet and the section update is simplified.

At the outlet the static pressure is fixed while density and momentum are extrapolated from the interior point. Static temperature is calculated from eq.1 and used to update the internal energy (eq.3). The quantity $\bar{e}$ is then evaluated. In case of supersonic inlet all the variables are extrapolated at the outflow.

Wall boundary conditions

The cell-vertex finite volume technique is directly applied at the wall boundary points using a half control volume for the point lying on the surface. When viscous flows are computed the non slip condition at the wall is implemented and the adiabatic wall ($\partial T / \partial n = 0$) is enforced using the neighboring points to the wall. Boundary orthogonal grids are used (Cravero, 1997). When inviscid flows are computed the slip condition for velocity at the wall point is introduced. This is done by deleting the diffusive flow vectors F_v, G_v (eq.8) and the convective flow vectors F, G are modified setting to zero the mass flow and energy fluxes at the wall boundary and by computing momentum exchange with static pressure only (Cravero-Satta, 1995b).

APPLICATIONS

It was found rather difficult to identify a proper case to test the code directly in a turbomachinery geometry. Therefore preliminary 1D and 2D calculations have been performed and compared to existing analytical solutions or other numerical results. Both are for high temperature air. The first illustration of the method is for one-dimensional transonic flow in a convergent-divergent duct for which the obtained results can be compared with those by Anderson (1992) with a different numerical method using a curve fitting procedure to interpolate the gas thermodynamic state from experimental tables. The fluid is equilibrium air. The calculation is performed setting an inlet total temperature of 1966 [K] and a ratio of outlet static pressure to inlet total pressure equal to 0.63. In these conditions a transonic flow is found in the duct with a shock wave at x/L=0.71. In figs.8-9 the calculated distributions of Mach

number and static temperature are compared with the values obtained by Anderson (1992).
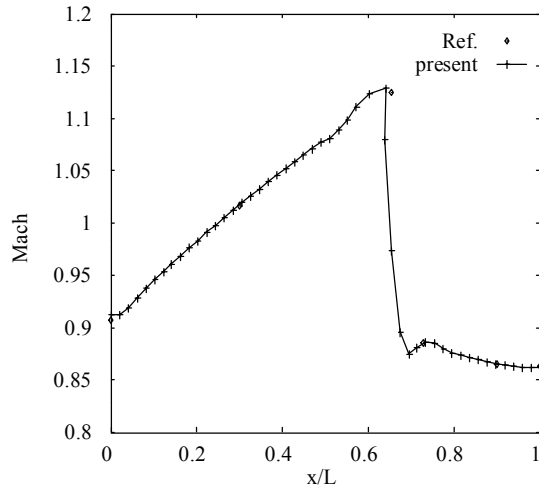
Fig.8: 1D case - Mach number distribution

A major disagreement between the ideal gas and the real gas computations is found on temperature distributions as confirmed in fig.9 where a difference of about 40 [K] is computed. This preliminary calculation has been useful mainly to verify the correct implementation of the inlet and outlet boundary conditions. Moreover the present solver, using a general equation of state, gives results comparable with those presented by Anderson using ad hoc interpolating functions for equilibrium air in the temperature range of interest; this is a quite interesting result because confirms that the proposed model can be directly applied to a particular problem without a need of special tuning for a particular substance.
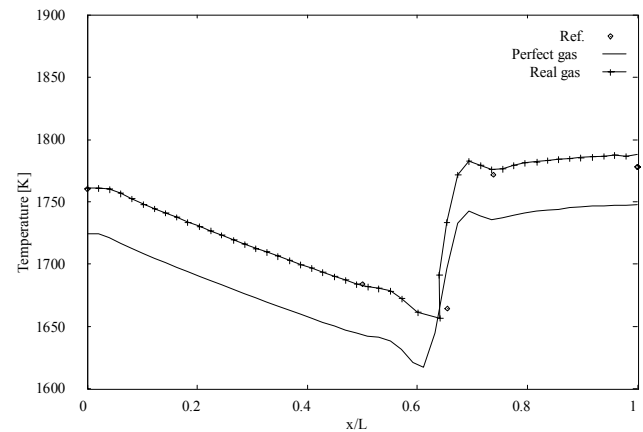
Fig.9: 1D case - Temperature distribution

The second test case consists of a two dimensional high temperature flow through a simple inlet. The inlet has a 10 deg. Wedge followed by a 10 deg. expansion and is symmetric about the centerline. A 201x51 grid was uniformly spaced in

6

Copyright (C) 2000 by ASME

the x-direction and slightly clustered near the wall in the y-direction; this same number of points had been used by Grossman et al. (1989). The inflow boundary is supersonic and a value of Mach number equal to 5.0 is fixed together with the following reference values: p= 0.101 [MPa], T= 3573 [K], ρ=0.0883 [kg/m^3]. All the variables are extrapolated at the outflow boundary. Inviscid flow condition is considered and appropriate boundary conditions are applied at the wall as previously described. Fig.10 presents the grid with the computed density shading to give an indication of the geometry and of the flow gradients due to the edges.
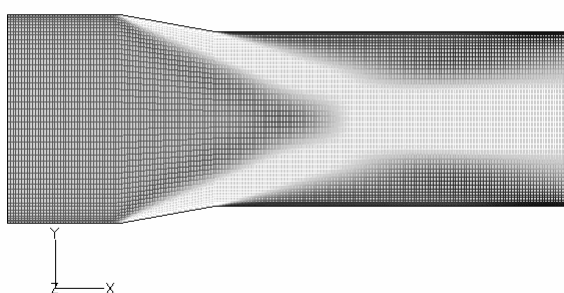
Fig.10: Supersonic inlet - 201x51 grid and density gradients
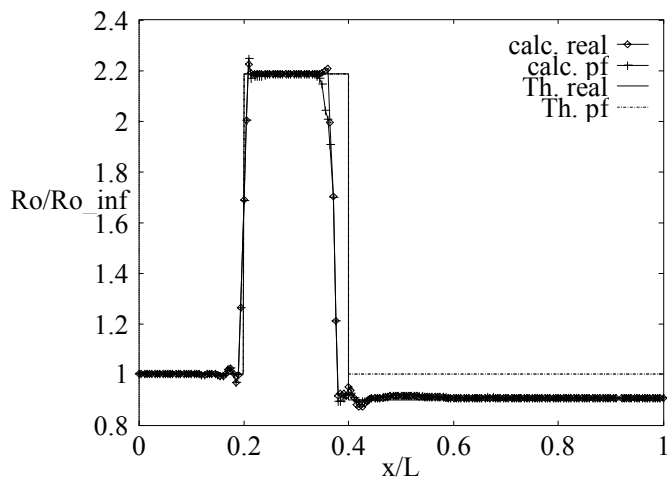
Fig.11: Supersonic wedge problem: surface density distributions

For this case theoretical solutions for equilibrium air exist (Grossman et al., 1989). Fig.11-12-13 compare numerical and theoretical predictions for density, pressure and temperature distributions for both perfect and real gas equations of state. In the above pictures the numerical predictions are shown using lines+crosses for the perfect gas case (calc.pf) and

lines+circles for the real gas case (calc.real); in the same pictures the theoretical results are shown using lines without symbols for the perfect gas case (Th.pf) and the real gas case (Th.real). The values are non-dimensional with respect to the inlet reference values.
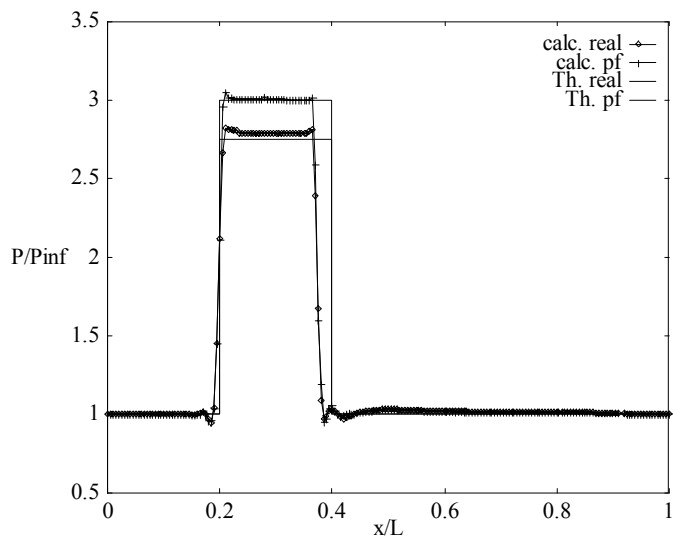
Fig.12: Supersonic wedge problem: surface pressure distributions
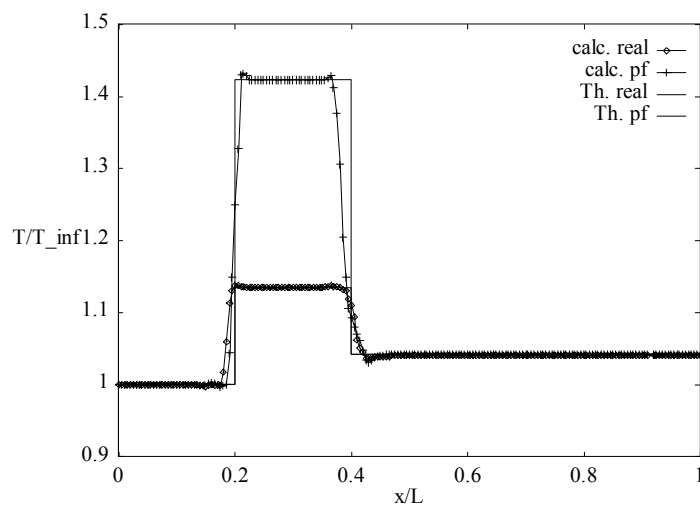
Fig.13 Supersonic wedge problem: surface temperature distributions

A general good agreement between the computed and the reference distributions can be observed. As can be seen from the above figures the computed distributions present overshooting and undershooting close to the shocks and the shocks are resolved in a few grid points with a little smearing. Actually to have a sharp and more precise shock resolution it is known that upwind or TVD methods should be considered (Hirsch, 1990). Nevertheless the final intent of the present

7   Copyright (C) 2000 by ASME

work is not to optimize a solver for shock resolution but to test the insertion of a real gas flow model into a Navier-Stokes solver to be used for industrial turbomachinery.

As can be seen a major discrepancy exists in the temperature prediction between the perfect and real gas model.
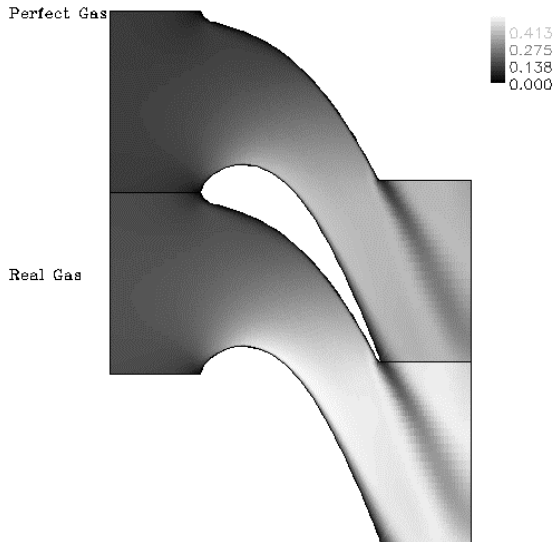
Fig. 14: Industrial turbine nozzle-Mach number shading

After the real gas CFD model validation, against available test cases, a preliminary Navier-Stokes calculation has been performed in an industrial steam turbine nozzle to asses the impact of the real fluid evaluation on the flowfield.
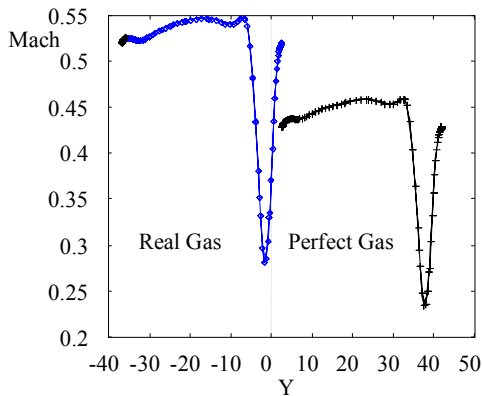
Fig.15: Industrial turbine nozzle-wake

An inlet total pressure of 10 [MPa] together with a zero inlet flow angle and an exit Mach number of 0.5 have been considered. In fig.14 a Mach number shading for both calculations (upper: perfect gas - lower: real gas) shows a different flow expansion. The difference between the two flowfields is also argued from fig.15 where the Mach number profiles in the wake region ($x/C_{ax}=1.3$) are compared.
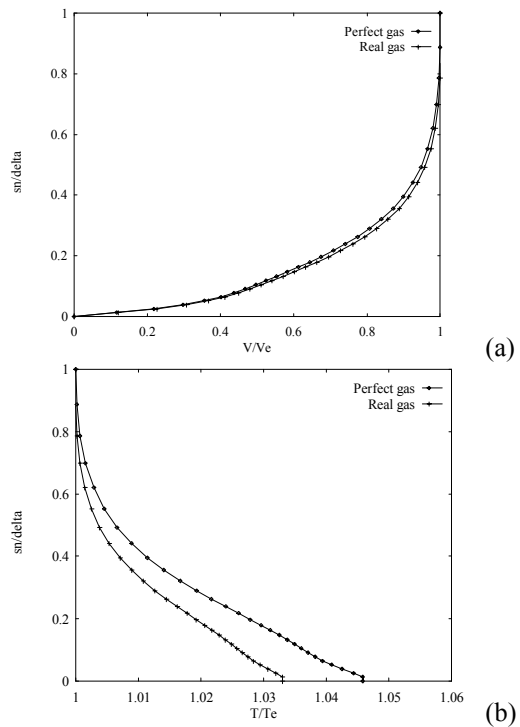
Fig.16: Suction side boundary layer at $x/Cax=0.62$ (a-velocity; b-temperature)
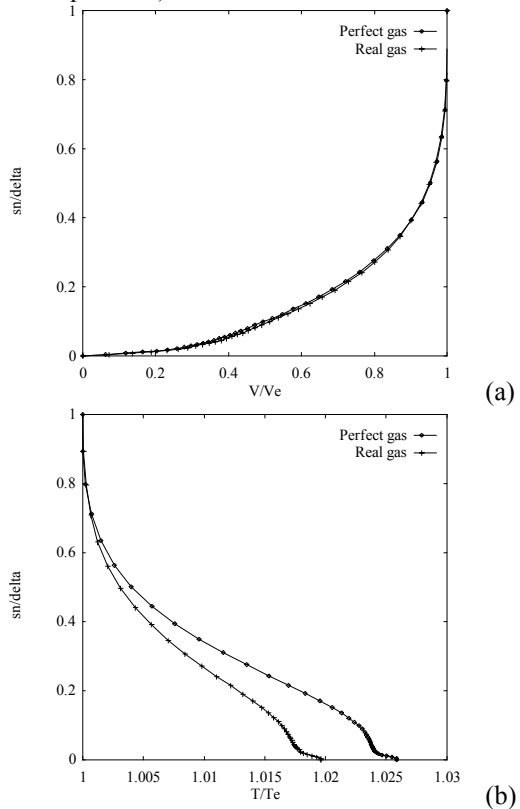
Fig.17: Suction side boundary layer at $x/Cax=0.87$ (a-velocity; b-temperature)

8

Copyright (C) 2000 by ASME

(a)

(b)
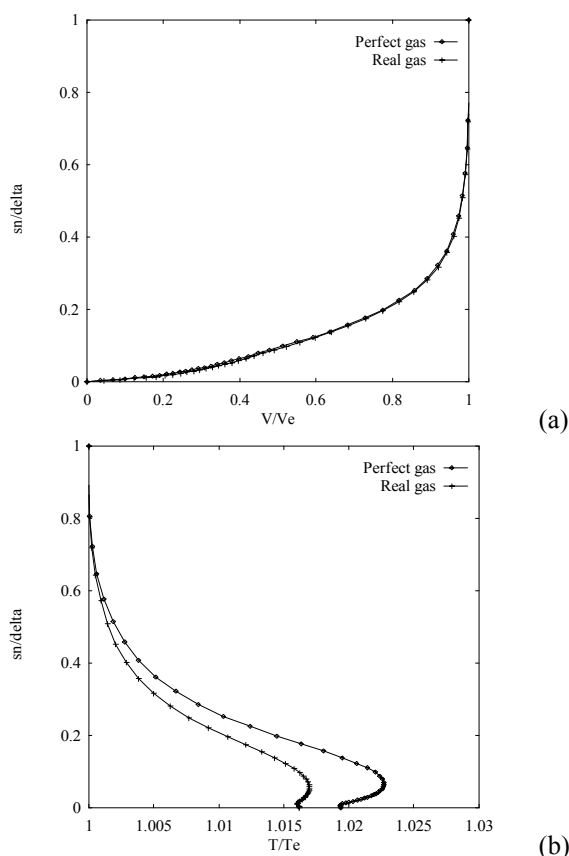
Fig.18: Suction side boundary layer at x/Cax=0.94 (a-velocity; b-temperature)

To have a deeper insight into the flowfield, several boundary layer profiles along the blade suction side obtained with the perfect gas assumption and the real gas model have been compared. Figs. 16-18 present the profiles of velocity and temperature at different locations along the blade suction side (x/Cax=0.62; x/Cax=0.87; x/Cax=0.94 respectively); in the above figures the local velocity and temperature are divided by the value external to the boundary layer and the normal distance from the wall (sn) is divided by the boundary layer thickness. It can be seen that the velocity distributions are not significantly influenced by the fluid model while the major changes are in the temperature profiles. The real fluid model predicts a lower temperature along the profile. This can give an explanation for the difference in the Mach number distributions (figs.14-15).

CONCLUSIONS

The RKA equation of state, when compared to experimental data for cryogenic hydrogen and steam, has shown good accuracy in the range of temperature and pressure interesting for turbomachinery applications. Some fundamental thermodynamic relations have been analytically derived using the RKA equation and presented in the paper. By computing the ratio of total to static temperature and pressure it can be verified that the ideal gas and the real fluid model differ appreciably and they do not show a unique trend of variation when different fluids are considered. This enforces the need for a real fluid model when temperature and pressure are outside the standard range for an ideal gas model. The real gas model has been implemented into an existing time-marching Navier-Stokes code previously developed by the authors for turbomachinery flow analysis with perfect gases (Chiari et al., 1998). The main modifications to the solver have been introduced into the inlet and outlet boundary conditions as described in the paper. The code, and model, validation has been made against other calculations (with different models) for high temperature equilibrium air, because of the lack of experimental data available for turbomachinery flows with real gas effects. The main advantages of the proposed CFD model are its flexibility in handling different fluids (the RKA equation requires a few number of external data to identify the fluid) and the robustness of the cell-vertex time-marching technique, that can be directly applied to a wide range of flows (from supersonic to low subsonic conditions). A preliminary Navier-Stokes calculation for an industrial turbine blade row has shown that the real gas effect can be detectable mainly on temperature and this affects the corresponding Mach number field.

AKNOWLEDGMENTS

REFERENCES

Abgral R., 1991, "An extension of Roe's upwind scheme to algebraic equilibrium real gas models", Computers and Fluids, vol.19 n.2, pp171-182;

Abbott M.M., Van Hess H.C., 1972, "Thermodynamics", McGraw Hill,;

Anderson, J. M., 1992, "Numerical Simulation of imperfect Gas Flows", PhD Thesis, University of Glasgow (UK).

Aungier R.H., 1995, "A Fast, Accurate Real Gas Equation of State for Fluid Dynamic Analysis Applications", ASME J. of Fluid Eng., vol.117;

Baldwin B.S., Lomax H., 1978, "Thin layer approximation and algebraic model for separated turbulent flows", AIAA paper 78-257;

Bober W., Chow W.L., 1990, "Nonideal isentropic gas flow through converging-diverging nozzles", ASME J. of Fluids Eng., vol.112, pp. 455-461;

Chiari P., Cravero C., Satta A., 1998, "A code for Navier-Stokes equations integration in 2D turbomachinery cascades" (in Italian), IMSE Internal Report 3/98, University of Genoa;

9

Cravero C., Satta A., 1995a, "Three-dimensional numerical solutions of turbomachinery annular cascade flow", ASME Cogen Turbo Power, Vienna, Austria, August;

Cravero C., Satta A., 1995b, "An algorithm for the numerical computation of convective fluxes in a finite volume method for complex configurations", Fluid Machinery Forum, ASME Summer Meeting, Hilton Head, USA, August;

Cravero C., 1997, "Boundary orthogonal grid generation by integrating a biharmonic system" (in Italian), 15th UIT National Heat Transfer Conference, June 19-20, Torino (Italy);

Denton J.D., 1978, "Throughflow calculations for transonic axial flow turbines", ASME J. for Gas Turbines and Power, vol.100;

Glaister P., 1988, "An approximate linearised Riemann solver for the Euler equations for real gases", J. Comp. Physics, vol.74, pp.382-408;

Grossman, B, Walters, R.W., 1989, "Analysis of flux-split algorithms for Euler's equations with real gases", AIAA Journal vol.27 n.5, pp.524-531;

Hall R.M., 1980, "Real-gas effects I - simulation of ideal gas flow by cryogenic nitrogen and other selected gases", AGARD LS 111, VKI, Belgium;

Hirsch, C., 1990, "Numerical computation of internal and external flows", vol.2, J. Wiley and Sons Ltd;

Kirillin V.A., Sychev V.V., Sheindlin A.E., 1987, "Engineering Thermodynamics", Mir Publisher, Moscow;

Johnson R.C.,1965,"Real Gas effects in critical-flow-through Nozzles and tabulated thermodynamic Properties", NASA TN D-2565, Washington DC.

Liou M.S., VanLeer B., Shuen J.S., 1990, "Splitting of inviscid fluxes for real gases", J. Comp. Physics, vol.87, pp.1-24;

McCarty R.H., 1975, "An hydrogen Technological Survey: Thermophysical Properties", NASA SP 3089, NASA Lewis Center.

Patek J., 1996, "Functional forms to describe thermodynamic properties of gases for fast calculations", ASME J. for Gas Turbines and Power, vol.118, pp.210-213;

Srinivasan S., Tannehill J.C., Weilmuenster K.J., 1987, "Simplified curve fits for the thermodynamic properties of equilibrium air", NASA Ref. Publication 1181;

Sullivan D.A., 1981, "Historical review of real-fluid isentropic flow models", ASME J. of Fluids Eng., vol.103, pp.258-267;

Suresh A., Liou M.S., 1991, "Osher's scheme for real gases", AIAA Journal, vol.29 n.6, pp.920-926;

Vinokur M., Montagné J.L:, 1990, "Generalized flux-vector splitting and Roe average for an equilibrium real gas", J. Comp. Physics, vol.89, pp.276-300;

Young J.B., 1988, "An equation of state for steam for turbomachinery and other flow calculations", ASME J. for Gas Turbines and Power, vol.110, pp.1-7;